PNAS
www.pnas.org

Supplementary Information for

Extracellular Vesicle Fibrinogen Induces Encephalitogenic CD8+ T cells in a Mouse Model of Multiple Sclerosis

Cory M. Willis[1], Alexandra M. Nicaise[1], Antoine Menoret[2,7], Jae Kyu Ryu[4], Andrew S. Mendiola[4], Evan R. Jellison[2], Maria I. Givogri[5], David Han[3], Ernesto R. Bongarzone[5], Katerina Akassoglou[4,6], Anthony T. Vella[2], and Stephen J. Crocker[1]*

Departments of Neuroscience[1], Immunology[2], and Cell Biology[3]
University of Connecticut School of Medicine, Farmington, CT;
[4]Gladstone Institutes, San Francisco, CA;
[5]Department of Anatomy and Cell Biology, University of Illinois at Chicago, Chicago, IL;
[6]Department of Neurology, University of California, San Francisco, San Francisco, CA
[7]Institute for Systems Genomics, UConn Health, Farmington, CT

Stephen J. Crocker
Email: crocker@uchc.edu

This PDF file includes:

Extended Materials and Methods

Animals. Mice were housed under a 12:12 light/dark cycle, 55 ± 5% relative humidity, and a temperature of 20 ± 2°C with access to standard laboratory chow and water *ad libitum*. They were housed in social groups of a maximum of 5 mice each in standard mouse housing cages and bedding.

Experimental Autoimmune Encephalomyelitis (EAE) was induced in C57B/6 male mice (8-12 week old) by immunizing with a 1:1 ratio of myelin oligodendrocyte glycoprotein (MOG35-55, AnaSpec Inc., Fremont, CA) dissolved in deionized water and complete Freund's adjuvant (CFA, Sigma, St. Louis, MO) containing 0.5 mg of Mycobacterium tuberculosis H37RA (Difco Laboratories: BD Diagnostics, Franklin Lakes, NJ), as described in previous studies (1,2). The MOG-CFA emulsion was administered subcutaneously (s.c.) into the flanks of the hind-limbs (300 μg/mouse). On days 0 and 2, pertussis toxin (PTX, List Biological, Campbell, CA) was injected intraperitoneally (i.p.) (500 ng/mouse). Weights and clinical scores were recorded daily by an experimenter blinded to experimental treatment of subjects. Clinical signs of disease severity were: 0, no clinical signs; 0.5, distal tail limpness; 1, full tail atony; 2, hind-limb paresis; 3, unilateral hind-limb paralysis; 4, bilateral hind-limb paralysis; 5, moribund.

CD8 and Isotype antibody injections. 500 µg of either **α**CD8 (*InVivo*MAb anti-mouse CD8 [Lyt 2.1, Clone: 116-13.1 (HB-129)], Bio X Cell, West Lebanon, New Hampshire) or **α**CD8-isotype antibody (*InVivo*MAb mouse IgG2a Isotype control [Clone: C1.18.4], Bio X Cell, West Lebanon, New Hampshire) in sterile PBS was injected intraperitoneally into pEV-injected MOG_{35-55}-EAE mice at peak clinical EAE and 5 days later.

Blood collection and pEV Isolation. Whole blood was centrifuged at 2000 x g for 15 min at room temperature and the upper plasma layer was drawn off. Plasma was centrifuged at 1500 x g at room temperature and the supernatant drawn off. Plasma samples were then subjected to a differential ultracentrifugation protocol for extracellular vesicle isolation as previously described (2). Briefly, plasma was spun at 12,000 x g for 30 min at 4°C. The supernatant was collected and equal amounts were subjected to ultracentrifugation at 150,000 x g for 90 min at 4°C. The supernatant was removed and the extracellular vesicle pellets were re-suspended in 150-200 µl of sterile, 0.22 µm filtered PBS and stored at -80°C until use. All samples were validated by electron microscopy.

Human Blood Samples. This study was approved by the Office for the Protection of Research Subjects at University of Illinois at Chicago and the Department of Defense Human Research Protection Office. All patients with MS were diagnosed with RRMS according to the revised McDonald criteria. At the time of blood collection, all patients with RRMS were in remission. All patients with MS were under interferon-beta treatment. Three milliliters of blood was collected in tubes with 0.5M ethylenediaminetetraacetic acid (Fisher Scientific, EDTA). Blood was pre-spun at 1500 x *g* for 15 mins at room temperature to isolate plasma. Plasma was then spun at 12,000 x *g* for 30 minutes to remove contaminating microvesicles and flash-frozen on dry ice until extracellular vesicle isolation.

Western Blotting. pEV preparations from either mouse or healthy human subjects or RRMS patient plasma were lysed in RIPA buffer (with protease inhibitor cocktail; Sigma) and separated on a pre-cast 12% Gel (Bio-Rad) by SDS-PAGE. Proteins were transferred to nitrocellulose and immunoblotted using unconjugated antisera against fibrinogen (Dako; catalog ID: A0080; 1:2500), fibrinogen alpha chain

(Abnova; catalog ID: H00002243-D01P; 1:1000), and the EV marker flotillin-1 (BD Biosciences; Clone 18/Flotillin-1, catalog ID: 610820, 1:500) that were then visualized by HRP-conjugated secondary antisera (Vector Laboratories, 1:1000-5000) using chemiluminescence (Clarity Western ECL; Bio-Rad). Images were captured using a ChemiDoc XRS+ imaging system (Bio-Rad). Human plasma plasminogen-depleted fibrinogen (Millipore-Sigma, catalog ID: 341578) or mouse plasma plasminogen-depleted plasma fibrinogen (Abcam, catalog ID: ab92791) (100 ng) were used as positive controls for the identification of fibrinogen chains on pEVs.

Quantitative Real-time Polymerase Chain Reaction (qRT-PCR). Total RNA was isolated from saline-perfused unfixed whole brain tissue using TRI Reagent (Sigma) according to the manufacturer's protocol. cDNA was amplified using the iScript kit (BioRad) and qPCR was performed using specific validated primer pairs for *Cxcl10* and *Ccl2* (Integrated DNA Technologies, Coralville, IA) and using the SsoAdvanced™ Universal SYBR® Green Supermix (BioRad) according to the manufacturer's protocol. Target cDNA was amplified and analyzed by the CFX Connect™ Real-Time PCR Detection System (BioRad). Primers for β-actin were used to assess the general expression level of the housekeeping gene among samples. The relative expression of target RNA was calculated using the comparative cycle threshold analysis (ΔΔCT).

Cytometry by time of flight (CyTOF). The four samples were permeabilized with methanol and incubated with Fc receptor blocking solution and a 31 heavy-metal conjugated antibody panel, including seven signaling markers, as previously described20. DNA was labeled using Cell-ID Intercalator-Ir. The samples were spiked with normalization beads and analyzed by a mass cytometer (HELIOS, Fluidigm) at Jackson Laboratories (Farmington, CT). The data were debarcoded using the Fluidigm Debarcoder v1.04. A single-cell and live-cell gate were identified in each sample. The

samples were downsampled to ensure equal numbers of cells per sample for ViSNE analysis (FlowJo, FlowJo, LLC) (3).

Immunohistochemistry. Spinal cord samples were collected and fixed 4% paraformaldehyde for 24 hours. Tissues were embedded in paraffin and 8 µm sections were applied to superfrost plus glass slides. Antigen retrieval was performed by heating sections to 90ºC in 0.1M citrate acid buffer for nine minutes. Slides were blocked in 10% normal goat serum (Millipore-Sigma). Sections were incubated with the following primary antibodies αCD8 (Bio X Cell, [Lyt 2.1, Clone: 116-13.1 (HB-129)], catalog ID: BE0118, 1:1000; Abcam, catalog ID: ab4055, 1:200), CD4 (Abcam, [clone: EPR19514], catalog ID: ab183685, 1:1000), CD68 (Abcam, [clone: FA-11], catalog ID: ab53444, 1:500), and Neurofilament M (Abcam, [clone: NF-09], catalog ID: ab7794, 1:500) in blocking buffer overnight at 4ºC. Sections were washed then incubated with the appropriate fluorescence conjugated secondary antibody (Invitrogen, 1:1000) for one hour at room temperature. Sections were washed and stained with FluoroMyelin green fluorescent myelin stain (Invitrogen, catalog ID: F34651, 1:300) for 20 minutes at room temperature. Sections were washed with PBS and counterstained with DAPI (Millipore-Sigma, 1:1000) for 10 minutes at room temperature. Sections were then mounted in Fluoromount-G (Southern Biotech). Quantification of immunopositive cells was performed on at least four spinal cord sections per animal (n = 3 subjects per treatment group / 12 total sections per antibody per subject) by an observer that was blinded to the experimental treatments. Number of positive cells were averaged per experimental subject and statistical comparisons between experimental treatment groups were performed using a Welch's t-test on account of unequal variances. Sections were imaged on an Olympus IX71 and processed using ImageJ software (National Institutes of Health).

Electron Microscopy. For negative staining, 20 µl drops of pEVs (in PBS) were adsorbed onto activated copper grids with carbon coating (Electron Microscopy Sciences) for 15 min, washed by dabbing the grid onto three drops of deionized water, and stained with 1% uranyl acetate (Electron Microscopy Sciences) for 1 min. Grids were imaged under a Hitachi H-7650 transmission electron microscope. For immunogold labeling, 20 µl of isolated pEVs were adsorbed onto activated nickel grids with carbon coating for 15 min. Grids were then blocked for 10 min on 100 µl drops of blocking buffer (1% NGS in PBS). Grids were then incubated for 60 minutes at room temperature on 25 µl drops of primary antibody against fibrinogen (Dako, catalog ID: A0080, 1:10 dilution in 1% NGS) and flotillin-1 (BD Biosciences, Clone 18/Flotillin-1, catalog ID: 610820, 1:10 dilution in 1% NGS). Grids were washed on 100 µl droplets of PBS three times for 5 min, blocked in 1% NGS for 5 min, and incubated with the appropriate secondary antibody conjugated with 15 nm gold particles or 10 nm gold particles (Electron Microscopy Sciences; 1:15 dilution in blocking solution) for 60 minutes, respectively. Grids were washed three times for 5 min in PBS followed by successive deionized water washes and counter-stained with 25 µl of 1% uranyl-acetate for 1 min. Excess uranyl-acetate was removed by gently blotting the grids which were then left to air dry before imaging under a transmission electron microscope.

In solution Protein Digestion. Extracellular vesicle pellets were resuspended in 1XRIPA buffer containing Halt Protease Inhibitor Cocktail (ThermoScientific, Waltham, MA; Prod# 87786). Samples were homogenized by sonication, and cleared by centrifugation at 14,000 rpm, 4°C, 10 min on a desktop centrifuge. Proteins were extracted by Chloroform/Methanol precipitation using established protocols. Protein pellets were dissolved and denatured in 8M urea, 0.4M ammonium bicarbonate, pH 8. The proteins were reduced by the addition of 1/10 volume of 45mM dithiothreitol (Pierce

ThermoScientific, catalog ID: 20290) and incubation at 37ºC for 20 minutes, then alkylated with the addition of 1/10 volume of 100mM iodoacetamide (Millipore-Sigma, catalog ID: I1149) with incubation in the dark at room temperature for 20 minutes. The urea concentration was adjusted to 2M by the addition of water prior to enzymatic digestion at 37°C with LysC (Wako, catalog ID: 125-05061) for 4 hours, then trypsin (Promega; Seq. Grade Mod. Trypsin, catalog ID: V5113) for an additional 16 hours. Protease:protein ratios were estimated at 1:50. Samples were acidified by the addition of 20% trifluoroacetic acid, then desalted using C18 MacroSpin columns (The Nest Group, catalog ID: SMM SS18V) following the manufacturer's directions with peptides eluted with 0.1% TFA, 80% acetonitrile. Eluted sample was speedvaced dry and dissolved in MS loading buffer (2% aceotonitrile, 0.2% trifluoroacetic acid). A nanodrop measurement (Thermo Scientific Nanodrop 2000 UV-Vis Spectrophotometer) determined protein concentrations (A260/A280). Each sample was then further diluted with MS loading buffer to 0.08μg/μl, with 0.4ug (5μl) injected for LC-MS/MS analysis.

LC-MS/MS on the Thermo Scientific Q Exactive Plus. LC-MS/MS analysis was performed on a Thermo Scientific Q Exactive Plus with a Waters nanoAcquity UPLC system, using a Waters Symmetry® C18 180μm x 20mm trap column and a ACQUITY UPLC PST (BEH) C18 nanoACQUITY Column 1.7 μm, 75 μm x 250 mm (37ºC) for peptide separation. Trapping was done at 5μl/min, 97% Buffer A (100% water, 0.1% formic acid) for 3 min. Peptide separation was performed at 330 nl/min with Buffer A: 100% water, 0.1% formic acid and Buffer B: 100% acetonitrile, 0.1% formic acid. A linear gradient (90 minutes) was run with 3% buffer B at initial conditions; 5% B at 1 minute; 35% B at 50 minutes; 50% B at 60 minutes; 90% B at 65-70; and back to initial conditions at 71 minutes. MS was acquired in profile mode over the 300-1,700 m/z range using 1 microscan; 70,000 resolution; AGC target of 3E6; and a full max ion time of 45

ms. MS/MS was acquired in centroid mode using 1 microscan; 17,500 resolution; AGC target of 1E5; full max IT of 100 ms; 1.7 m/z isolation window; normalized collision energy of 28; and 200-2,000 m/z scan range. Up to 20 MS/MS were collected per MS scan on species with an intensity threshold of 2E4, charge states 2-6, peptide match preferred, and dynamic exclusion set to 20 seconds.

Peptide Identification. Data was analyzed using Proteome Discoverer software v2.2 (Thermo Scientific). Data searching was performed using the Mascot algorithm (version 2.6.0) (Matrix Science) against the SwissProtein database with taxonomy restricted Homo sapiens. The search parameters included tryptic peptides with up to 3 missed cleavages, 10 ppm precursor mass tolerance and 0.02 Da fragment mass tolerance, and variable (dynamic) modifications of methionine oxidation, carbamidomethylated cysteine, deamidated asparagine or glutamine, and citrullination of arginine. Normal and decoy database searches were run, with the confidence level set to 95% ($P < 0.05$). Scaffold (version Scaffold_4.8.7, Proteome Software Inc., Portland, OR) was used to validate MS/MS based peptide and protein identifications. Peptide identifications were accepted if they could be established at greater than 95.0% probability by the Scaffold Local FDR algorithm. Protein identifications were accepted if they could be established at greater than 99.0% probability and contained at least 2 identified peptides.

Extended Materials and Methods References

1. Frausto RF, Crocker SJ, Eam B, Whitmire JK, Whitton JL. Myelin oligodendrocyte glycoprotein peptide-induced experimental allergic encephalomyelitis and T cell responses are unaffected by immunoproteasome deficiency. Journal of neuroimmunology. 2007;192(1-2):124-33. PMCID: 2175388.
2. Willis CM, Menoret A, Jellison ER, Nicaise AM, Vella AT, Crocker SJ. A Refined Bead-Free Method to Identify Astrocytic Exosomes in Primary Glial Cultures and Blood Plasma. Frontiers in neuroscience. 2017;11:335. PMCID: PMC5471332.
3. Svedova J, Menoret A, Mittal P, Ryan JM, Buturla JA, Vella AT. Therapeutic blockade of CD54 attenuates pulmonary barrier damage in T cell-induced acute lung injury. American journal of physiology Lung cellular and molecular physiology. 2017;313(1):L177-l91.

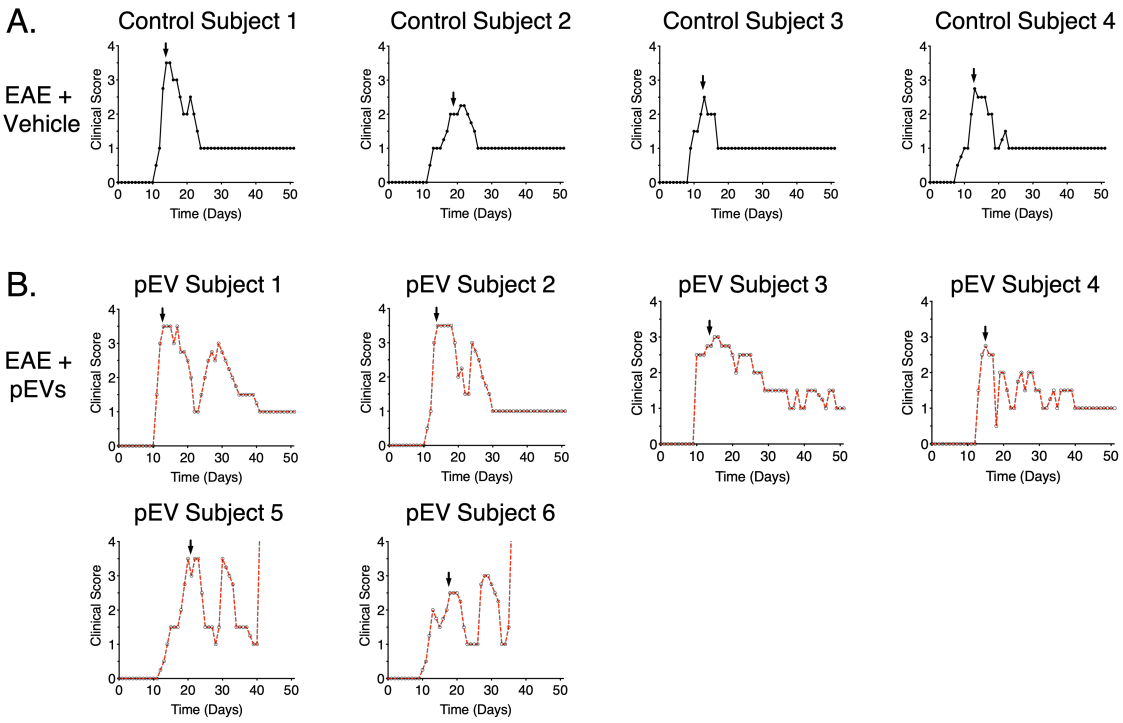

***SI Appendix* Fig. S1.** pEVs induced a spontaneous relapsing-remitting phenotype in wild-type C57BL/6 mice during MOG_{35-55}-induced EAE. *(A)* Clinical EAE disease courses in individual vehicle (n = 4) and *(B)* pEV-treated mice (n = 6). From grouped data in Fig. 1*D*.

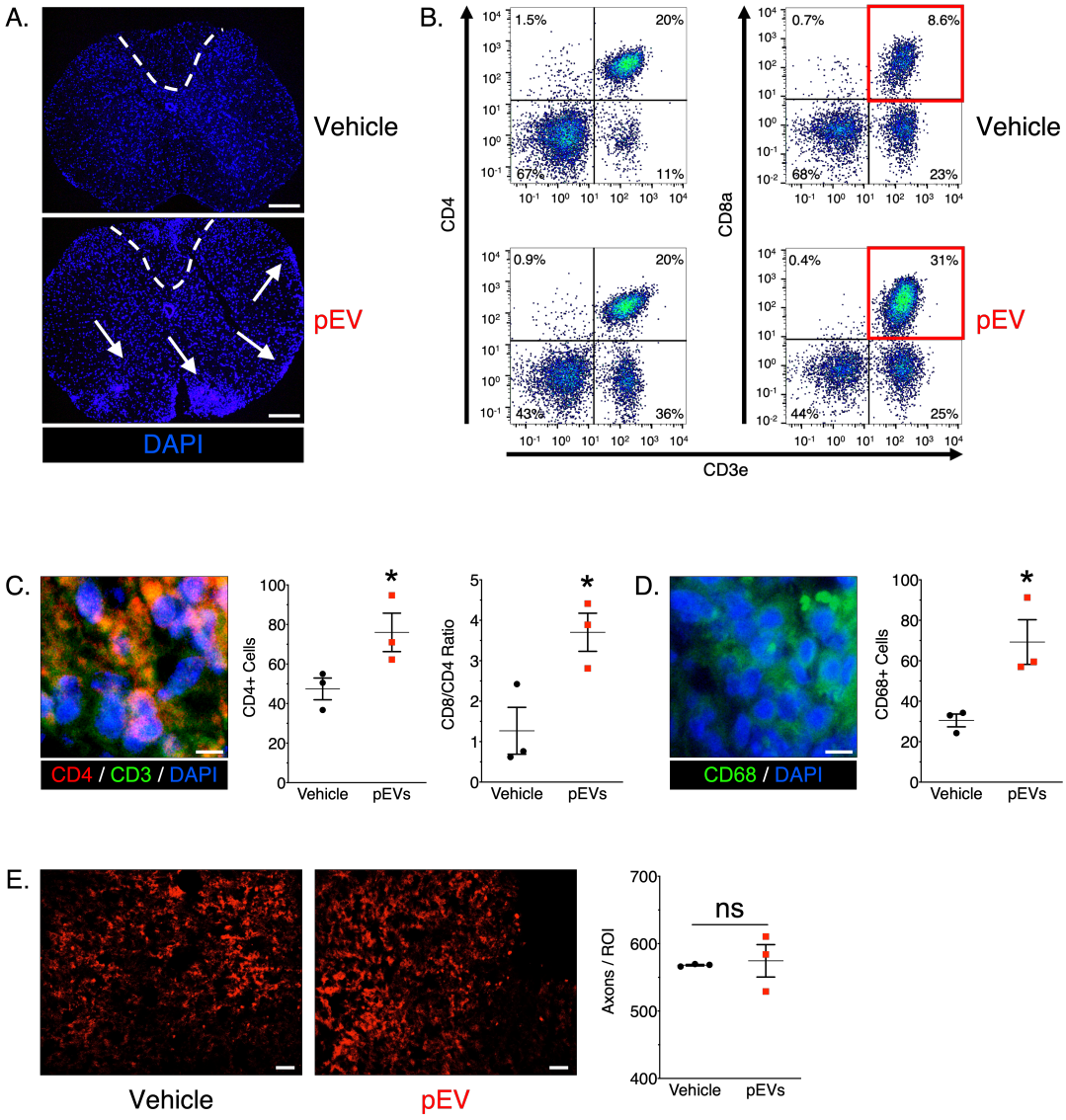

***SI Appendix* Fig. S2.**

***SI Appendix* Fig. S2.** Characterization of increased immune cell infiltrates and axonal injury in spinal cords of pEV-treated R/R EAE mice during spontaneous relapse.. (*A*) Low magnification representative image of spinal cord cross sections from vehicle-treated and pEV-treated EAE mice both collected at the same time of the first clinical relapse in pEV-treated mice. Sections were stained with DAPI and clearly indicate (arrows) notable differences in cellular infiltrates in the pEV-treated animals (*See* Fig. 2*H*). Dotted line demarcates the dorsal column which was used for immunohistological analyses. (*B*) Scatter plots of CD3+/CD4+ and CD3+/CD8+ T lymphocytes collected from spinal cord tissues of vehicle and pEV-treated EAE mice analyzed by CyTOF (*See* Fig. 2*C*). These analyses indicate that in pEV-treated animals 98.7% of CD8+ cells were also CD3+. CD8+/CD3+ T cells represented 55% of all infiltrating T cells in this treatment group at this time point while, CD8+ cells represented 27% of all CD3+ cells in vehicle treated animals. (*C*) Immunohistochemistry for CD8+ T cells demonstrated spatial co-localization within the demyelinated spinal cord (*See* Fig. 2*J*), and analysis of CD4+ T cells in the dorsal columns of vehicle and pEV-treated indicated a higher proportion of CD4+ immune cells within the infiltrates within this anatomical site in pEV-treated animals. These differences in CD8+ and CD4+ immune cells also reflected a higher ratio of CD8+ T cells in pEV treated animals than observed in vehicle-treated animals. (*D*) Analysis of CD68+ macrophages in the dorsal column of spinal cord tissues from pEV and vehicle treated animals also revealed a higher abundance of macrophages in the cellular infiltrates of pEV-treated mice. (*E*) Analysis of Neurofilament M in the dorsal columns of spinal cord tissues from pEV and vehicle treated mice determined comparable numbers of axons in both treatment groups indicating that at this time of the first clinical relapse, axon loss was not a significant pathological feature in the pEV-treated animals in spite of ongoing clinical EAE symptomatology. Scale bars: A = 1 mm; C,D, E = 20 µm.

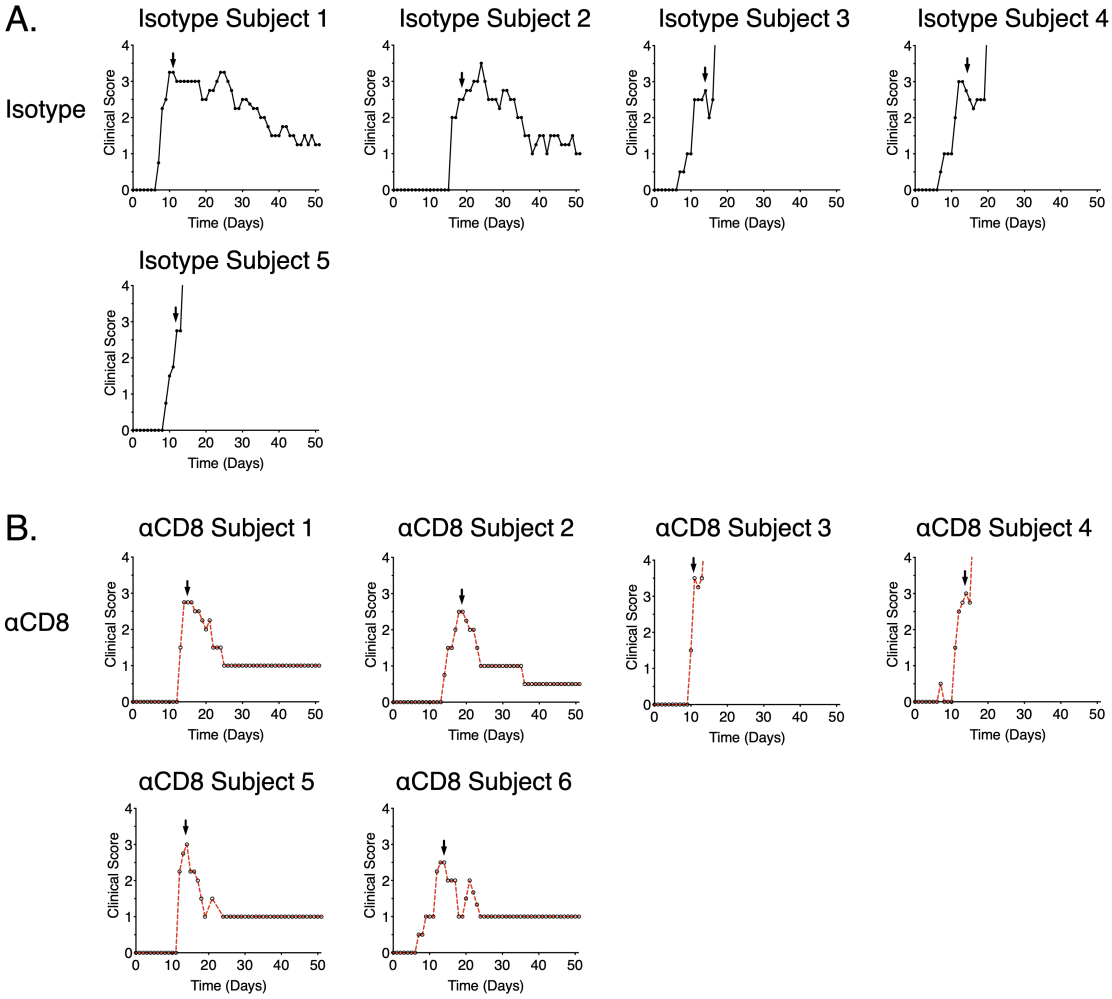

***SI Appendix* Fig. S3.** pEVs induce a CD8+ T-cell response responsible for the development of a spontaneous relapsing phenotype in MOG_{35-55}-EAE. *(A)* Clinical disease courses in individual isotype antisera (n = 4) and *(B)* αCD8 (n = 7) function blocking antibody-treated mice. From grouped data in Fig. 2*F*.

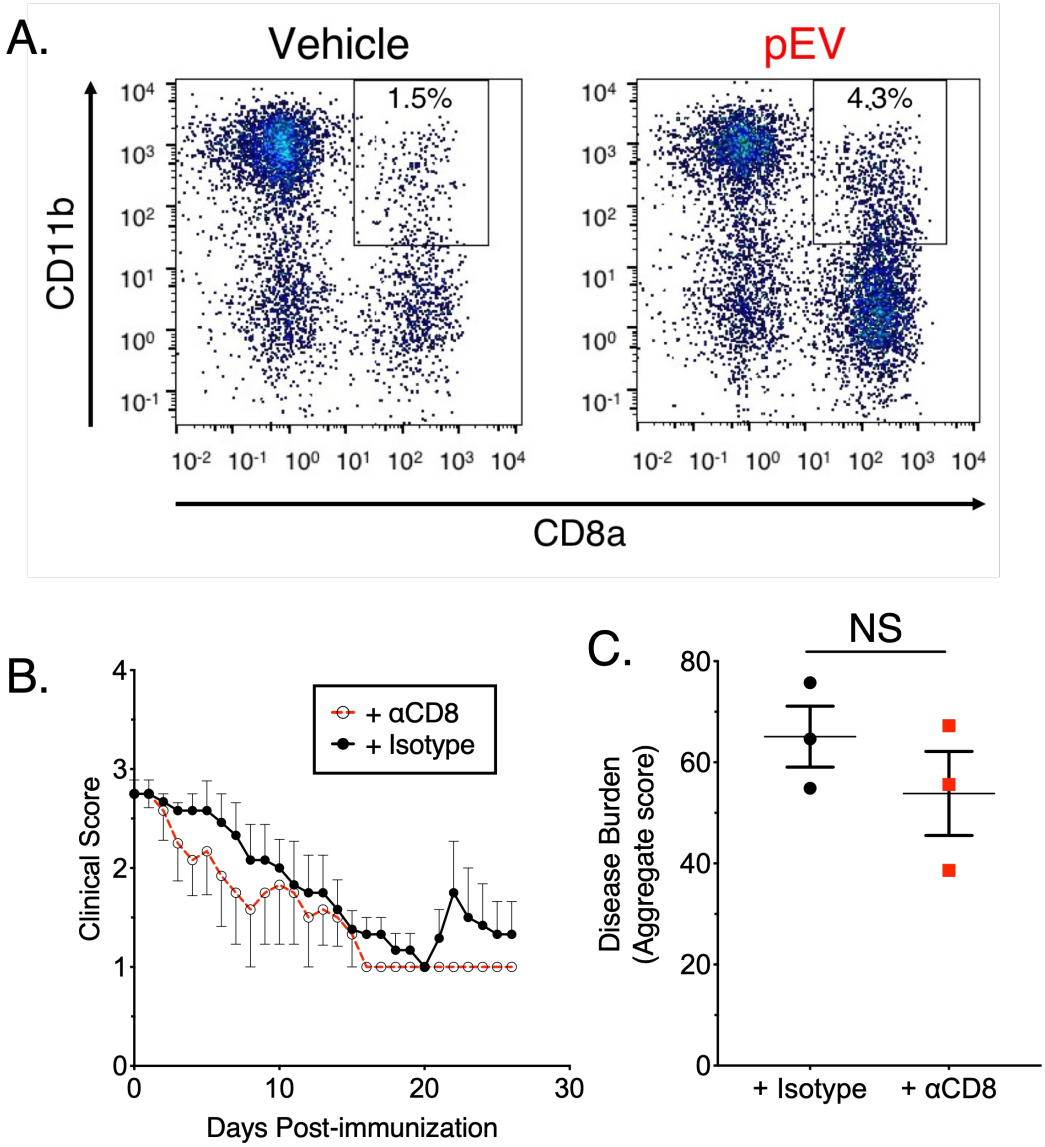

***SI Appendix* Fig. S4.** CyTOF Analysis of spinal cords at time of spontaneous relapses revealed a unique CD8+ T cell population. *(A)* pEV-R/R mice had increases in CD11b/ CD8+ immune cell infiltrates during a spontaneous relapse. *(B)* Administration of isotype antisera (n = 3) and αCD8 (n = 3) to MOG_{35-55}-EAE mice had no effect on clinical disease course and *(C)* disease burden. (Values are mean ± s.e.m., where $^*P < 0.05$ calculated by two-way ANOVA with uncorrected Fisher's LSD post-hoc test; $^*P < 0.05$ (Mann-Whitney *U* test.) Grouped data is the result of two independent experiments.

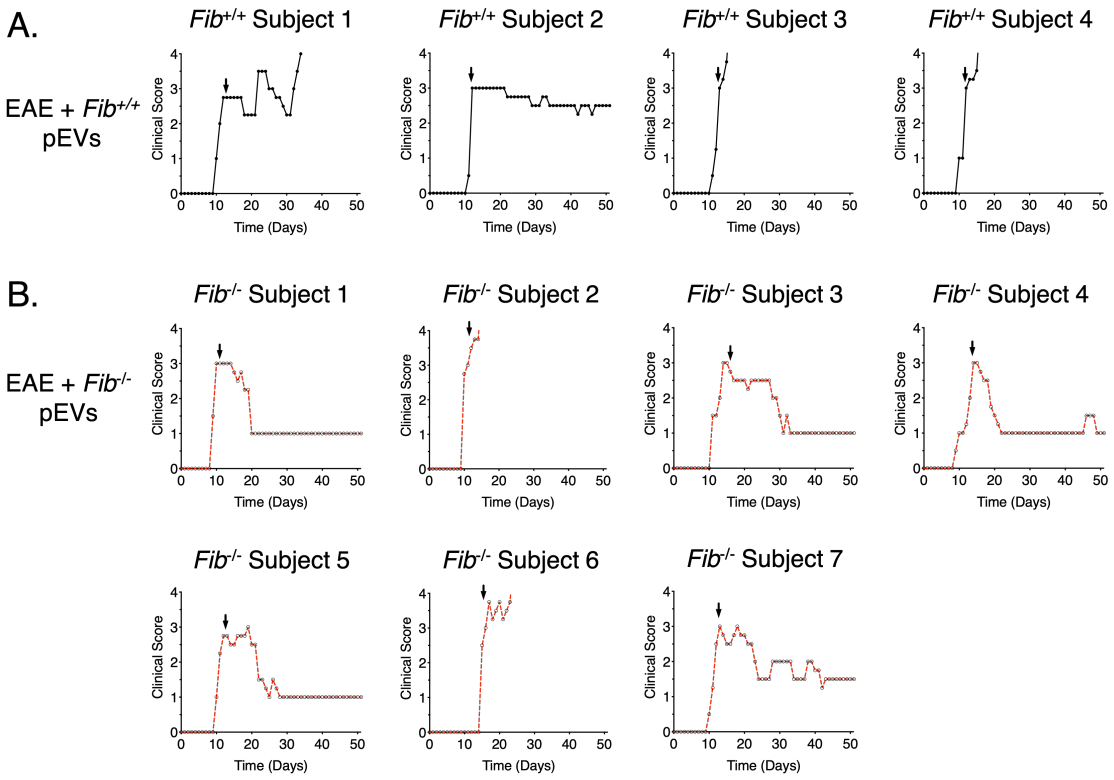

***SI Appendix* Fig. S5.** pEV fibrinogen is necessary to induce a spontaneous relapsing-remitting phenotype in wild-type C57BL/6 mice during MOG_{35-55}-induced EAE. *(A)* Clinical disease courses in individual MOG_{35-55}-EAE mice administered *Fib*$^{+/+}$ (n = 5) or *(B) Fib*$^{-/-}$ (n = 6) pEVs. From grouped data in Fig. 3*G*.

Table S1. List of LC-MS/MS peptides identified using PF-2D platform in sample in uniquely identified by Proteome software.

Expectation	Gene ID	Protein Name	MW	% Coverage	empai
0.00054	FIBA_MOUSE	Fibrinogen alpha chain	87375	12.3	0.05
170	PZP_MOUSE	Pregnancy zone protein	165748	2.6	0.03
420	LAMC1_MOUSE	Laminin subunit gamma-1	177185	0.7	
480	CO7A1_MOUSE	Collagen alpha-1(VII) chain	295054	0.8	
2400	DACT2_MOUSE	Dapper homolog 2	81617	1.3	

Table S2. LC-MS/MS Identified 265 proteins in pEVs from non-diseased and relapsing-remitting multiple sclerosis patients.

				Total Spectral Counts					
Entry Name	**Protein ID**	**MW**	**Alternate ID**	**Control #3**	**Control #13**	**Control #40**	**MS #39**	**MS #10**	**MS #2**
1433G_HUMAN	14-3-3 protein gamma	28 kDa	YWHAG	4	0	0	0	0	0
1433Z_HUMAN	14-3-3 protein zeta/delta	28 kDa	YWHAZ	5	0	1	3	0	1
A1AG1_HUMAN	Alpha-1-acid glycoprotein 1	24 kDa	ORM1	4	4	1	4	2	1
A1AG2_HUMAN	Alpha-1-acid glycoprotein 2	24 kDa	ORM2	11	10	14	12	10	4
A1AT_HUMAN	Alpha-1-antitrypsin	47 kDa	SERPINA1	118	86	62	108	96	85
A1BG_HUMAN	Alpha-1B-glycoprotein	54 kDa	A1BG	23	19	19	25	18	18
A2AP_HUMAN	Alpha-2-antiplasmin	55 kDa	SERPINF2	17	12	7	14	13	11
A2GL_HUMAN	Leucine-rich alpha-2-glycoprotein	38 kDa	LRG1	7	1	1	7	3	2
A2MG_HUMAN	Alpha-2-macroglobulin	163 kDa	A2M	1526	1320	920	774	1468	1323
AACT_HUMAN	Alpha-1-antichymotrypsin	48 kDa	SERPINA3	38	26	16	33	24	25
ACTB_HUMAN	Actin, cytoplasmic 1	42 kDa	ACTB	24	2	14	28	2	17
ACTC_HUMAN	Actin, alpha cardiac muscle 1	42 kDa	ACTC1	14	0	8	12	1	6
ACTN1_HUMAN	Alpha-actinin-1	103 kDa	ACTN1	7	0	2	15	0	5
AFAM_HUMAN	Afamin	69 kDa	AFM	18	14	9	20	12	10
ALBU_HUMAN	Serum albumin	69 kDa	ALB	1498	976	720	960	635	969
ALS_HUMAN	Insulin-like growth factor-binding protein complex acid labile subunit	66 kDa	IGFALS	14	6	2	4	1	9
AMBP_HUMAN	Protein AMBP	39 kDa	AMBP	22	14	11	15	20	12
ANGT_HUMAN	Angiotensinogen	53 kDa	AGT	19	16	11	15	12	15
ANT3_HUMAN	Antithrombin-III	53 kDa	SERPINC1	29	22	13	37	13	20
APOA_HUMAN	Apolipoprotein(a)	501 kDa	LPA	4	0	7	37	4	0
APOA1_HUMAN	Apolipoprotein A-I	31 kDa	APOA1	164	51	55	62	43	51
APOA2_HUMAN	Apolipoprotein A-II	11 kDa	APOA2	25	14	19	20	13	15
APOA4_HUMAN	Apolipoprotein A-IV	45 kDa	APOA4	52	21	16	20	14	18
APOB_HUMAN	Apolipoprotein B-100	516 kDa	APOB	607	222	253	417	202	144
APOC1_HUMAN	Apolipoprotein C-I	9 kDa	APOC1	5	3	3	7	5	4
APOC2_HUMAN	Apolipoprotein C-II	11 kDa	APOC2	6	3	5	7	4	4
APOC3_HUMAN	Apolipoprotein C-III	11 kDa	APOC3	9	3	2	5	2	3
APOD_HUMAN	Apolipoprotein D	21 kDa	APOD	13	8	6	10	2	6
APOE_HUMAN	Apolipoprotein E	36 kDa	APOE	16	14	12	15	13	13
APOF_HUMAN	Apolipoprotein F	35 kDa	APOF	6	4	1	5	2	1
APOH_HUMAN	Beta-2-glycoprotein 1	38 kDa	APOH	39	12	13	20	13	16
APOL1_HUMAN	Apolipoprotein L1	44 kDa	APOL1	8	8	16	8	19	5
APOM_HUMAN	Apolipoprotein M	21 kDa	APOM	10	1	2	3	0	1
ATRN_HUMAN	Attractin	159 kDa	ATRN	3	2	1	2	0	0
C1QA_HUMAN	Complement C1q subcomponent subunit A	26 kDa	C1QA	7	9	5	5	7	6
C1QB_HUMAN	Complement C1q subcomponent subunit B	27 kDa	C1QB	25	25	21	10	22	15
C1QC_HUMAN	Complement C1q subcomponent subunit C	26 kDa	C1QC	7	11	10	5	10	8
C1R_HUMAN	Complement C1r subcomponent	80 kDa	C1R	24	29	25	28	41	25
C1RL_HUMAN	Complement C1r subcomponent-like protein	53 kDa	C1RL	0	0	0	0	3	0
C1S_HUMAN	Complement C1s subcomponent	77 kDa	C1S	6	6	4	6	9	6
C4BPA_HUMAN	C4b-binding protein alpha chain	67 kDa	C4BPA	73	75	58	92	94	61
C4BPB_HUMAN	C4b-binding protein beta chain	28 kDa	C4BPB	9	9	9	10	13	10
CAP1_HUMAN	Adenylyl cyclase-associated protein 1	52 kDa	CAP1	0	0	0	3	0	0
CBG_HUMAN	Corticosteroid-binding globulin	45 kDa	SERPINA6	5	4	0	3	0	0
CBPB2_HUMAN	Carboxypeptidase B2	48 kDa	CPB2	1	7	3	0	2	2
Entry Name	**Protein ID**	**MW**	**Alternate ID**	**Control #3**	**Control #13**	**Control #40**	**MS #39**	**MS #10**	**MS #2**
CBPN_HUMAN	Carboxypeptidase N catalytic chain	52 kDa	CPN1	7	5	5	4	5	3
CD5L_HUMAN	CD5 antigen-like	38 kDa	CD5L	25	19	24	21	29	20
CD9_HUMAN	CD9 antigen	25 kDa	CD9	5	0	4	7	0	6
CERU_HUMAN	Ceruloplasmin	122 kDa	CP	91	54	51	73	56	56
CFAB_HUMAN	Complement factor B	86 kDa	CFB	34	19	19	32	21	21
CFAH_HUMAN	Complement factor H	139 kDa	CFH	80	92	88	96	96	63
CFAI_HUMAN	Complement factor I	66 kDa	CFI	12	11	9	13	14	8
CHLE_HUMAN	Cholinesterase	68 kDa	BCHE	3	0	1	0	1	0
CLH1_HUMAN	Clathrin heavy chain 1	192 kDa	CLTC	0	0	0	4	0	0
CLUS_HUMAN	Clusterin	52 kDa	CLU	24	16	17	26	17	17
CNDP1_HUMAN	Beta-Ala-His dipeptidase	57 kDa	CNDP1	3	0	0	10	0	2
CO2_HUMAN	Complement C2	83 kDa	C2	3	2	0	1	0	0
CO3_HUMAN	Complement C3	187 kDa	C3	500	447	389	388	538	469
CO4A_HUMAN	Complement C4-A	193 kDa	C4A	217	157	150	206	273	201
CO4B_HUMAN	Complement C4-B	193 kDa	C4B	217	163	143	204	263	199
CO5_HUMAN	Complement C5	188 kDa	C5	61	72	50	70	72	53
CO6_HUMAN	Complement component C6	105 kDa	C6	11	16	10	17	18	16
CO7_HUMAN	Complement component C7	94 kDa	C7	12	19	10	10	18	8
CO8A_HUMAN	Complement component C8 alpha chain	65 kDa	C8A	12	14	9	13	14	12
CO8B_HUMAN	Complement component C8 beta chain	67 kDa	C8B	28	24	24	16	31	23
CO8G_HUMAN	Complement component C8 gamma chain	22 kDa	C8G	7	6	8	6	10	5
CO9_HUMAN	Complement component C9	63 kDa	C9	16	13	10	18	26	14
COF1_HUMAN	Cofilin-1	19 kDa	CFL1	3	0	1	6	0	3
COF2_HUMAN	Cofilin-2	19 kDa	CFL2	0	0	1	2	0	1
COL11_HUMAN	Collectin-11	29 kDa	COLEC11	1	4	0	0	1	2
COR1A_HUMAN	Coronin-1A	51 kDa	CORO1A	0	0	0	4	0	0
CPN2_HUMAN	Carboxypeptidase N subunit 2	61 kDa	CPN2	9	7	10	11	12	6
CXCL7_HUMAN	Platelet basic protein	14 kDa	PPBP	0	0	0	2	0	0
ECM1_HUMAN	Extracellular matrix protein 1	61 kDa	ECM1	3	15	5	3	2	5
ENOA_HUMAN	Alpha-enolase	47 kDa	ENO1	1	0	0	2	0	0
F13A_HUMAN	Coagulation factor XIII A chain	83 kDa	F13A1	4	20	17	38	7	13
F13B_HUMAN	Coagulation factor XIII B chain	76 kDa	F13B	0	17	14	26	3	5
FA12_HUMAN	Coagulation factor XII	68 kDa	F12	15	15	14	12	20	18
FA5_HUMAN	Coagulation factor V	252 kDa	F5	5	2	1	4	2	3
FA9_HUMAN	Coagulation factor IX	52 kDa	F9	2	0	0	0	1	0
FBLN1_HUMAN	Fibulin-1	77 kDa	FBLN1	13	8	2	6	4	6

FBLN3_HUMAN	EGF-containing fibulin-like extracellular matrix protein 1	55 kDa	EFEMP1	2	2	2	2	3	2
FCGBP_HUMAN	IgGFc-binding protein	572 kDa	FCGBP	3	2	6	16	12	2
FCN2_HUMAN	Ficolin-2	34 kDa	FCN2	2	2	1	1	1	0
FCN3_HUMAN	Ficolin-3	33 kDa	FCN3	14	11	6	4	20	7
FETUA_HUMAN	Alpha-2-HS-glycoprotein	39 kDa	AHSG	28	19	19	25	19	19
FETUB_HUMAN	Fetuin-B	42 kDa	FETUB	1	0	1	1	2	1
FHR1_HUMAN	Complement factor H-related protein 1	38 kDa	CFHR1	5	0	11	12	6	12
FHR2_HUMAN	Complement factor H-related protein 2	31 kDa	CFHR2	3	1	2	4	1	3
FHR3_HUMAN	Complement factor H-related protein 3	37 kDa	CFHR3	0	0	0	0	0	6
FIBA_HUMAN	Fibrinogen alpha chain	95 kDa	FGA	96	379	346	351	225	319
FIBB_HUMAN	Fibrinogen beta chain	56 kDa	FGB	140	853	872	829	612	758
FIBG_HUMAN	Fibrinogen gamma chain	52 kDa	FGG	123	465	426	388	334	408

Entry Name	Protein ID	MW	Alternate ID	Control #3	Control #13	Control #40	MS #39	MS #10	MS #2
FINC_HUMAN	Fibronectin	263 kDa	FN1	209	477	353	282	253	319
FLNA_HUMAN	Filamin-A	281 kDa	FLNA	3	0	5	75	1	2
FLNC_HUMAN	Filamin-C	291 kDa	FLNC	0	0	0	0	0	0
G3P_HUMAN	Glyceraldehyde-3-phosphate dehydrogenase	36 kDa	GAPDH	6	0	4	14	1	2
GELS_HUMAN	Gelsolin	86 kDa	GSN	40	45	35	34	42	31
GPX3_HUMAN	Glutathione peroxidase 3	26 kDa	GPX3	0	1	1	0	0	2
H2A1B_HUMAN	Histone H2A type 1-B/E	14 kDa	HIST1H2AB	0	0	0	4	0	0
H2B1B_HUMAN	Histone H2B type 1-B	14 kDa	HIST1H2BB	0	0	0	5	0	0
H4_HUMAN	Histone H4	11 kDa	HIST1H4A	0	0	0	3	0	1
HABP2_HUMAN	Hyaluronan-binding protein 2	63 kDa	HABP2	1	0	0	4	1	2
HBA_HUMAN	Hemoglobin subunit alpha	15 kDa	HBA1	43	17	23	18	31	23
HBB_HUMAN	Hemoglobin subunit beta	16 kDa	HBB	39	17	30	23	36	22
HBD_HUMAN	Hemoglobin subunit delta	16 kDa	HBD	15	4	10	8	12	6
HEMO_HUMAN	Hemopexin	52 kDa	HPX	55	39	29	37	29	39
HEP2_HUMAN	Heparin cofactor 2	57 kDa	SERPIND1	20	13	10	11	15	14
HGFA_HUMAN	Hepatocyte growth factor activator	71 kDa	HGFAC	3	2	3	1	7	3
HGFL_HUMAN	Hepatocyte growth factor-like protein	80 kDa	MST1	1	3	0	0	1	0
HPT_HUMAN	Haptoglobin	45 kDa	HP	154	63	73	123	111	125
HPTR_HUMAN	Haptoglobin-related protein	39 kDa	HPR	85	52	63	75	93	77
HRG_HUMAN	Histidine-rich glycoprotein	60 kDa	HRG	30	29	30	30	29	25
HV102_HUMAN	Immunoglobulin heavy variable 1-2	13 kDa	IGHV1-2	1	0	1	2	4	1
HV103_HUMAN	Immunoglobulin heavy variable 1-3	13 kDa	IGHV1-3	2	5	2	1	1	3
HV108_HUMAN	Immunoglobulin heavy variable 1-8	13 kDa	IGHV1-8	0	0	0	0	0	2
HV118_HUMAN	Immunoglobulin heavy variable 1-18	13 kDa	IGHV1-18	2	2	0	3	3	2
HV146_HUMAN	Immunoglobulin heavy variable 1-46	13 kDa	IGHV1-46	3	5	2	1	3	3
HV205_HUMAN	Immunoglobulin heavy variable 2-5	13 kDa	IGHV2-5	7	5	3	4	5	5
HV226_HUMAN	Immunoglobulin heavy variable 2-26	13 kDa	IGHV2-26	3	0	2	1	2	2
HV307_HUMAN	Immunoglobulin heavy variable 3-7	13 kDa	IGHV3-7	8	6	8	7	11	0
HV309_HUMAN	Immunoglobulin heavy variable 3-9	13 kDa	IGHV3-9	12	5	12	5	10	9
HV311_HUMAN	Immunoglobulin heavy variable 3-11	13 kDa	IGHV3-11	8	0	0	0	0	0
HV313_HUMAN	Immunoglobulin heavy variable 3-13	13 kDa	IGHV3-13	6	4	8	0	6	6
HV315_HUMAN	Immunoglobulin heavy variable 3-15	13 kDa	IGHV3-15	4	3	4	2	3	2
HV321_HUMAN	Immunoglobulin heavy variable 3-21	13 kDa	IGHV3-21	0	6	0	0	0	0
HV323_HUMAN	Immunoglobulin heavy variable 3-23	13 kDa	IGHV3-23	7	8	7	4	7	8
HV330_HUMAN	Immunoglobulin heavy variable 3-30	13 kDa	IGHV3-30	8	10	8	6	11	9
HV349_HUMAN	Immunoglobulin heavy variable 3-49	13 kDa	IGHV3-49	3	2	1	4	5	2
HV372_HUMAN	Immunoglobulin heavy variable 3-72	13 kDa	IGHV3-72	2	4	6	4	5	2
HV373_HUMAN	Immunoglobulin heavy variable 3-73	13 kDa	IGHV3-73	1	1	1	0	2	0
HV374_HUMAN	Immunoglobulin heavy variable 3-74	13 kDa	IGHV3-74	7	8	4	6	8	9
HV404_HUMAN	Immunoglobulin heavy variable 4-4	13 kDa	IGHV4-4	0	5	0	0	0	0
HV428_HUMAN	Immunoglobulin heavy variable 4-28	13 kDa	IGHV4-28	2	0	1	0	1	1
HV432_HUMAN	Immunoglobulin heavy variable 4-30-2	13 kDa	IGHV4-30-2	8	5	7	4	6	0
HV434_HUMAN	Immunoglobulin heavy variable 4-34	14 kDa	IGHV4-34	11	9	9	7	8	7
HV551_HUMAN	Immunoglobulin heavy variable 5-51	13 kDa	IGHV5-51	9	10	3	5	6	2
HV5X1_HUMAN	Immunoglobulin heavy variable 5-10-1	13 kDa	IGHV5-10-1	3	4	2	2	4	2
HV601_HUMAN	Immunoglobulin heavy variable 6-1	13 kDa	IGHV6-1	1	1	0	0	2	1
HV64D_HUMAN	Immunoglobulin heavy variable 3-64D	?		3	2	3	1	2	1
HV741_HUMAN	Immunoglobulin heavy variable 7-4-1	13 kDa	IGHV7-4-1	0	0	0	0	4	5

Entry Name	Protein ID	MW	Alternate ID	Control #3	Control #13	Control #40	MS #39	MS #10	MS #2
IC1_HUMAN	Plasma protease C1 inhibitor	55 kDa	SERPING1	19	16	8	18	12	8
IGA2_HUMAN	Immunoglobulin alpha-2 heavy chain	49 kDa		29	23	15	24	30	15
IGD_HUMAN	Immunoglobulin delta heavy chain	56 kDa		2	6	2	1	25	2
IGG1_HUMAN	Immunoglobulin gamma-1 heavy chain	49 kDa		317	127	133	171	128	146
IGHA1_HUMAN	Immunoglobulin heavy constant alpha 1	38 kDa	IGHA1	104	95	78	96	126	64
IGHD_HUMAN	Immunoglobulin heavy constant delta	42 kDa	IGHD	0	5	0	0	22	0
IGHG2_HUMAN	Immunoglobulin heavy constant gamma 2	36 kDa	IGHG2	194	120	96	108	97	99
IGHG3_HUMAN	Immunoglobulin heavy constant gamma 3	41 kDa	IGHG3	101	74	71	60	84	51
IGHG4_HUMAN	Immunoglobulin heavy constant gamma 4	36 kDa	IGHG4	62	39	51	34	30	47
IGHM_HUMAN	Immunoglobulin heavy constant mu	49 kDa	IGHM	361	264	388	239	484	266
IGJ_HUMAN	Immunoglobulin J chain	18 kDa	JCHAIN	16	11	19	16	20	13
IGK_HUMAN	Immunoglobulin kappa light chain	23 kDa		173	124	137	111	137	98
IGKC_HUMAN	Immunoglobulin kappa constant	12 kDa	IGKC	191	132	149	119	144	111
IGL1_HUMAN	Immunoglobulin lambda-1 light chain	23 kDa		116	70	75	75	109	53
IGLC2_HUMAN	Immunoglobulin lambda constant 2	11 kDa	IGLC2	126	79	96	88	109	62
IGLC7_HUMAN	Immunoglobulin lambda constant 7	11 kDa	IGLC7	47	39	49	36	37	33
IGM_HUMAN	Immunoglobulin mu heavy chain	63 kDa		303	238	331	211	393	247
ILK_HUMAN	Integrin-linked protein kinase	51 kDa	ILK	2	0	0	6	0	0
ITA2B_HUMAN	Integrin alpha-IIb	113 kDa	ITGA2B	5	0	5	18	0	10
ITB3_HUMAN	Integrin beta-3	87 kDa	ITGB3	5	0	3	14	0	5
ITIH1_HUMAN	Inter-alpha-trypsin inhibitor heavy chain H1	101 kDa	ITIH1	44	32	25	29	28	20
ITIH2_HUMAN	Inter-alpha-trypsin inhibitor heavy chain H2	106 kDa	ITIH2	47	31	27	35	28	31
ITIH3_HUMAN	Inter-alpha-trypsin inhibitor heavy chain H3	100 kDa	ITIH3	4	0	0	6	0	0
ITIH4_HUMAN	Inter-alpha-trypsin inhibitor heavy chain H4	103 kDa	ITIH4	35	32	23	46	27	33
K1C10_HUMAN	Keratin, type I cytoskeletal 10	59 kDa	KRT10	1	4	0	0	1	1

K22E_HUMAN	Keratin, type II cytoskeletal 2 epidermal	65 kDa	KRT2	0	3	0	0	0	2
K2C1_HUMAN	Keratin, type II cytoskeletal 1	66 kDa	KRT1	2	5	0	0	0	2
KAIN_HUMAN	Kallistatin	49 kDa	SERPINA4	7	7	3	3	4	6
KLKB1_HUMAN	Plasma kallikrein	71 kDa	KLKB1	18	7	11	4	8	13
KNG1_HUMAN	Kininogen-1	72 kDa	KNG1	28	29	20	26	18	16
KPYM_HUMAN	Pyruvate kinase PKM	58 kDa	PKM	3	0	0	3	0	0
KV105_HUMAN	Immunoglobulin kappa variable 1-5	13 kDa	IGKV1-5	5	2	3	4	2	2
KV108_HUMAN	Immunoglobulin kappa variable 1-8	13 kDa	IGKV1-8	7	11	5	4	9	5
KV112_HUMAN	Immunoglobulin kappa variable 1-12	13 kDa	IGKV1-12	9	3	6	4	8	4
KV113_HUMAN	Immunoglobulin kappa variable 1-13	13 kDa	IGKV1-13	4	0	1	3	0	0
KV116_HUMAN	Immunoglobulin kappa variable 1-16	13 kDa	IGKV1-16	3	2	4	2	3	2
KV117_HUMAN	Immunoglobulin kappa variable 1-17	13 kDa	IGKV1-17	6	5	8	5	12	3
KV127_HUMAN	Immunoglobulin kappa variable 1-27	13 kDa	IGKV1-27	7	13	4	3	6	3
KV139_HUMAN	Immunoglobulin kappa variable 1-39	13 kDa	IGKV1-39	8	3	6	2	7	4
KV224_HUMAN	Immunoglobulin kappa variable 2-24	13 kDa	IGKV2-24	3	3	5	2	2	3
KV228_HUMAN	Immunoglobulin kappa variable 2-28	13 kDa	IGKV2-28	6	7	7	2	7	7
KV229_HUMAN	Immunoglobulin kappa variable 2-29	13 kDa	IGKV2-29	0	2	3	0	0	0
KV230_HUMAN	Immunoglobulin kappa variable 2-30	13 kDa	IGKV2-30	4	4	5	2	3	3
KV240_HUMAN	Immunoglobulin kappa variable 2-40	13 kDa	IGKV2-40	4	3	5	2	3	2
KV311_HUMAN	Immunoglobulin kappa variable 3-11	13 kDa	IGKV3-11	9	4	3	4	4	4
KV315_HUMAN	Immunoglobulin kappa variable 3-15	12 kDa	IGKV3-15	3	2	5	2	4	3
KV320_HUMAN	Immunoglobulin kappa variable 3-20	13 kDa	IGKV3-20	10	8	11	11	12	7
KV401_HUMAN	Immunoglobulin kappa variable 4-1	13 kDa	IGKV4-1	8	6	4	5	5	5

Entry Name	Protein ID	MW	Alternate ID	Control #3	Control #13	Control #40	MS #39	MS #10	MS #2
KVD15_HUMAN	Immunoglobulin kappa variable 3D-15	13 kDa	IGKV3D-15	3	3	5	3	4	3
KVD20_HUMAN	Immunoglobulin kappa variable 3D-20	13 kDa	IGKV3D-20	9	4	7	11	8	6
KVD29_HUMAN	Immunoglobulin kappa variable 2D-29	13 kDa	IGKV2D-29	0	2	3	0	2	0
LBP_HUMAN	Lipopolysaccharide-binding protein	53 kDa	LBP	3	1	1	4	8	4
LDHB_HUMAN	L-lactate dehydrogenase B chain	37 kDa	LDHB	2	0	0	1	0	0
LG3BP_HUMAN	Galectin-3-binding protein	65 kDa	LGALS3BP	21	14	18	19	33	20
LIMS1_HUMAN	LIM and senescent cell antigen-like-containing domain protein 1	37 kDa	LIMS1	0	0	1	2	0	0
LV144_HUMAN	Immunoglobulin lambda variable 1-44	12 kDa	IGLV1-44	4	4	1	0	3	0
LV147_HUMAN	Immunoglobulin lambda variable 1-47	12 kDa	IGLV1-47	6	4	3	2	4	2
LV151_HUMAN	Immunoglobulin lambda variable 1-51	12 kDa	IGLV1-51	2	2	2	2	3	2
LV211_HUMAN	Immunoglobulin lambda variable 2-11	13 kDa	IGLV2-11	1	3	2	1	2	1
LV218_HUMAN	Immunoglobulin lambda variable 2-18	12 kDa	IGLV2-18	2	0	1	0	2	0
LV301_HUMAN	Immunoglobulin lambda variable 3-1	12 kDa	IGLV3-1	0	0	0	0	3	0
LV310_HUMAN	Immunoglobulin lambda variable 3-10	12 kDa	IGLV3-10	2	4	2	2	3	3
LV319_HUMAN	Immunoglobulin lambda variable 3-19	12 kDa	IGLV3-19	2	0	1	1	1	1
LV321_HUMAN	Immunoglobulin lambda variable 3-21	12 kDa	IGLV3-21	3	4	4	1	3	2
LV39_HUMAN	Immunoglobulin lambda variable 3-9	?		3	4	0	0	2	1
LV861_HUMAN	Immunoglobulin lambda variable 8-61	13 kDa	IGLV8-61	2	1	3	1	0	1
LV949_HUMAN	Immunoglobulin lambda variable 9-49	13 kDa	IGLV9-49	0	2	0	0	0	0
LYSC_HUMAN	Lysozyme C	17 kDa	LYZ	1	1	0	1	2	1
MASP1_HUMAN	Mannan-binding lectin serine protease 1	79 kDa	MASP1	2	0	0	0	0	0
MMRN1_HUMAN	Multimerin-1	138 kDa	MMRN1	0	0	0	2	0	0
MYH9_HUMAN	Myosin-9	227 kDa	MYH9	2	0	1	24	3	0
MYL6_HUMAN	Myosin light polypeptide 6	17 kDa	MYL6	1	0	1	5	0	1
PARVB_HUMAN	Beta-parvin	42 kDa	PARVB	3	0	0	1	0	0
PDLI1_HUMAN	PDZ and LIM domain protein 1	36 kDa	PDLIM1	0	0	0	5	0	0
PEDF_HUMAN	Pigment epithelium-derived factor	46 kDa	SERPINF1	7	7	5	4	4	8
PF4V_HUMAN	Platelet factor 4 variant	12 kDa	PF4V1	5	0	5	4	2	3
PGRP2_HUMAN	N-acetylmuramoyl-L-alanine amidase	62 kDa	PGLYRP2	18	14	15	12	15	14
PHLD_HUMAN	Phosphatidylinositol-glycan-specific phospholipase D	92 kDa	GPLD1	0	4	4	4	2	0
PIGR_HUMAN	Polymeric immunoglobulin receptor	83 kDa	PIGR	1	1	9	3	12	4
PLEK_HUMAN	Pleckstrin	40 kDa	PLEK	5	0	0	5	0	3
PLF4_HUMAN	Platelet factor 4	11 kDa	PF4	6	0	6	4	3	4
PLMN_HUMAN	Plasminogen	91 kDa	PLG	65	111	91	79	64	80
PLTP_HUMAN	Phospholipid transfer protein	55 kDa	PLTP	4	0	0	0	0	0
PON1_HUMAN	Serum paraoxonase/arylesterase 1	40 kDa	PON1	32	18	22	28	8	22
POTEE_HUMAN	POTE ankyrin domain family member E	121 kDa	POTEE	11	0	5	13	0	7
POTEJ_HUMAN	POTE ankyrin domain family member J	117 kDa	POTEJ	0	0	0	7	0	0
PPIA_HUMAN	Peptidyl-prolyl cis-trans isomerase A	18 kDa	PPIA	1	0	1	2	0	0
PRG4_HUMAN	Proteoglycan 4	151 kDa	PRG4	1	0	3	0	1	6
PROF1_HUMAN	Profilin-1	15 kDa	PFN1	2	0	0	3	0	2
PROP_HUMAN	Properdin	51 kDa	CFP	1	4	3	2	4	1
PROS_HUMAN	Vitamin K-dependent protein S	75 kDa	PROS1	24	27	23	24	34	30
PZP_HUMAN	Pregnancy zone protein	164 kDa	PZP	269	235	196	206	259	287
RAP1A_HUMAN	Ras-related protein Rap-1A	21 kDa	RAP1A	2	0	2	3	0	1
RET4_HUMAN	Retinol-binding protein 4	23 kDa	RBP4	15	6	7	4	4	5
SAA4_HUMAN	Serum amyloid A-4 protein	15 kDa	SAA4	9	0	3	7	0	1
SAMP_HUMAN	Serum amyloid P-component	25 kDa	APCS	13	13	11	13	17	12

Entry Name	Protein ID	MW	Alternate ID	Control #3	Control #13	Control #40	MS #39	MS #10	MS #2
SEPP1_HUMAN	Selenoprotein P	43 kDa	SELENOP	6	2	3	2	4	3
SHBG_HUMAN	Sex hormone-binding globulin	44 kDa	SHBG	3	0	0	0	0	1
STOM_HUMAN	Erythrocyte band 7 integral membrane protein	32 kDa	STOM	0	0	0	2	0	0
TBA1B_HUMAN	Tubulin alpha-1B chain	50 kDa	TUBA1B	6	0	1	19	0	0
TBA4A_HUMAN	Tubulin alpha-4A chain	50 kDa	TUBA4A	4	0	1	19	0	0
TBA8_HUMAN	Tubulin alpha-8 chain	50 kDa	TUBA8	4	0	0	13	0	0
TBB1_HUMAN	Tubulin beta-1 chain	50 kDa	TUBB1	3	0	1	9	0	0
TBB4B_HUMAN	Tubulin beta-4B chain	50 kDa	TUBB4B	1	0	1	18	0	0
TBB5_HUMAN	Tubulin beta chain	50 kDa	TUBB	1	0	1	21	0	0
TERA_HUMAN	Transitional endoplasmic reticulum ATPase	89 kDa	VCP	1	0	0	9	0	6
TETN_HUMAN	Tetranectin	23 kDa	CLEC3B	5	6	0	2	0	0
TFR1_HUMAN	Transferrin receptor protein 1	85 kDa	TFRC	0	0	0	0	0	4
THBG_HUMAN	Thyroxine-binding globulin	46 kDa	SERPINA7	1	1	2	0	3	0
THRB_HUMAN	Prothrombin	70 kDa	F2	43	47	45	41	49	45

TLN1_HUMAN	Talin-1	270 kDa	TLN1	48	0	27	154	4	56
TLN2_HUMAN	Talin-2	272 kDa	TLN2	0	0	0	0	0	0
TPM4_HUMAN	Tropomyosin alpha-4 chain	29 kDa	TPM4	2	0	0	0	0	0
TRFE_HUMAN	Serotransferrin	77 kDa	TF	179	123	117	151	102	154
TSP1_HUMAN	Thrombospondin-1	129 kDa	THBS1	6	0	2	36	5	11
TTHY_HUMAN	Transthyretin	16 kDa	TTR	41	24	27	28	24	29
URP2_HUMAN	Fermitin family homolog 3	76 kDa	FERMT3	5	0	1	8	0	0
VINC_HUMAN	Vinculin	124 kDa	VCL	6	0	1	15	0	1
VTDB_HUMAN	Vitamin D-binding protein	53 kDa	GC	61	34	33	49	27	46
VTNC_HUMAN	Vitronectin	54 kDa	VTN	25	21	17	24	22	20
VWF_HUMAN	von Willebrand factor	309 kDa	VWF	3	118	60	77	65	78
WDR1_HUMAN	WD repeat-containing protein 1	66 kDa	WDR1	4	0	0	2	0	0
ZA2G_HUMAN	Zinc-alpha-2-glycoprotein	34 kDa	AZGP1	5	2	2	4	2	2
ZYX_HUMAN	Zyxin	61 kDa	ZYX	3	0	0	4	0	1

Table S3. Demographic and Clinical Features of Patients with RRMS and Non-Diseased Controls

Patient ID	Gender	Age	Disease	EDSS	DMT
3	Male	58	--	--	--
13	Female	48	--	--	--
40	Female	46	--	--	--
39	Female	45	RRMS	0	IFN-β
10	Male	53	RRMS	5	IFN-β
2	Female	48	RRMS	6.5	IFN-β